

## $J/\psi$ photoproduction in ultra-peripheral Pb-Pb and p-Pb collisions with the ALICE detector

Jaroslav Adam *for the ALICE collaboration*

*Faculty of Nuclear Sciences and Physical Engineering  
Czech Technical University in Prague*

### Abstract

Ultra-relativistic heavy ions generate strong electromagnetic fields which offer the possibility to study gamma-gamma, gamma-nucleus and gamma-proton processes at the LHC in ultra-peripheral Pb-Pb and p-Pb collisions (UPC). Exclusive photoproduction of  $J/\psi$  vector mesons is sensitive to the gluon distribution of the interacting target (proton or nucleus). This process is expected to be sensitive to saturation phenomena and nuclear gluon shadowing. Here we report on the ALICE measurement of  $J/\psi$  coherent photoproduction in Pb-Pb UPC at  $\sqrt{s_{NN}} = 2.76$  TeV at forward and central rapidities. Furthermore, we also present results on the  $J/\psi$  photoproduction in p-Pb UPC at  $\sqrt{s_{NN}} = 5.02$  TeV in the forward and backward rapidities, where the rapidity is measured in the laboratory frame with respect to the proton beam direction. The  $J/\psi$  mesons have been identified through their leptonic decays.

### Keywords:

photoproduction, ultra-peripheral collision, gluon saturation, nuclear gluon shadowing

### 1. Introduction

Photoproduction reactions of photons on protons or lead nuclei,  $\gamma p \rightarrow J/\psi p$  and  $\gamma Pb \rightarrow J/\psi Pb$ , which leave only a  $J/\psi$  meson as a new particle in the final state, allow the study of saturation phenomena and nuclear gluon shadowing at low Bjorken- $x$ . The cross section of exclusive photoproduction of  $J/\psi$  in LO pQCD is sensitive to the square of the gluon distribution in the target [1]. The ALICE experiment measured this process in  $\gamma p$  and  $\gamma Pb$  with ultra-peripheral p-Pb and Pb-Pb collisions (UPC).

The ultra-peripheral collision is a collision of Pb-ions at a distance larger than the sum of nuclear radii, or a collision of a proton and a Pb-ion at an impact parameter large enough to suppress hadronic interactions. Therefore the only interaction mechanism in both cases

is through the electromagnetic field, which behaves as a flux of virtual photons. The intensity of such a flux is proportional to the square of the electric charge.

Pb-Pb UPC allow us to study  $\gamma$ -Pb reactions, since both of the nuclei can be the source of virtual photons. In p-Pb, on the other hand, we measure  $\gamma p$  reactions because the Pb nucleus is most likely the photon source.

In p-Pb UPC, the centre-of-mass energy of the  $\gamma p$  system is  $W_{\gamma p}^2 = 2E_p M_{J/\psi} e^{-y}$ , where  $E_p$  is the proton beam energy,  $M_{J/\psi}$  is the mass of the  $J/\psi$  and  $y$  is the rapidity of the  $J/\psi$  along the direction of the proton beam. Higher values of  $W_{\gamma p}$  are reached at negative (backward) rapidity corresponding to a  $J/\psi$  produced in the direction opposite to that of the proton beam.

$J/\psi$  production in Au-Au UPC has been measured at RHIC [2]. Exclusive  $J/\psi$  production has been measured at HERA [3] [4] using ep collisions, at the Tevatron [5] in  $p\bar{p}$  collisions at mid-rapidity and recently by LHCb in pp collisions at forward rapidity [6].

The ALICE collaboration has measured coherent  $J/\psi$

*Email address:* [jaroslav.adam@cern.ch](mailto:jaroslav.adam@cern.ch) (Jaroslav Adam for the ALICE collaboration)

production at forward rapidities [7] and coherent and incoherent  $J/\psi$  production at mid-rapidities [8] in Pb-Pb UPC, and exclusive  $J/\psi$  photoproduction in p-Pb collisions at  $\sqrt{s_{NN}} = 5.02$  TeV [9].

## 2. The ALICE experiment at the LHC

The measurements reported here were performed with the ALICE central detectors, which cover the pseudorapidity range  $|\eta| < 0.9$ , and the forward muon spectrometer, covering the pseudorapidity interval  $-4.0 < \eta < -2.5$ <sup>1</sup>. Also important for UPC analyses are the forward scintillators VZERO-A and VZERO-C at pseudorapidity  $2.8 < \eta < 5.1$  and  $-3.7 < \eta < -1.7$  respectively and zero degree neutron and proton calorimeters (ZDC) with acceptance for neutrons of  $|\eta| < 8.8$  and for protons of  $6.5 < |\eta| < 7.5$  and  $-9.7^\circ < \phi < 9.7^\circ$ , where  $\phi$  is azimuthal angle of the particle.

The central tracking system is divided into an Inner Tracking System (ITS), Time Projection Chamber (TPC) and Time of Flight detector (TOF). The ITS is placed closest to the beam pipe, and is subdivided into 6 layers of tracking silicon detectors. The two innermost layers of the ITS, the Silicon Pixel Detectors (SPD), have acceptance extended up to  $|\eta| < 1.4$ . The TPC provides tracking and particle identification according to specific energy loss. The central detectors are surrounded by a large solenoid magnet of magnetic field  $B = 0.5$  T.

The muon spectrometer is composed of a composite absorber, 5 MWPC tracking stations, a trigger system and a dipole magnet creating an integrated field of 3 T·m.

The trigger inputs relevant for UPC analyses are provided by the SPD, TOF, VZERO detectors and the muon spectrometer.

## 3. Signal extraction for exclusive $J/\psi$ in p-Pb

The requirements on the data selection include no activity in SPD, VZERO-A and ZDCs, activity in VZERO-C compatible with the expected muons from beam-beam interaction and two unlike-sign tracks in the muon spectrometer passing the tracks quality selection. Candidates in a range in  $J/\psi$  rapidity produce a measurement at a given  $\langle W_{\gamma p} \rangle$ .

The direction of the beams in the LHC was inverted in order to measure dimuons in the forward  $2.5 < y <$

4.0 (p-Pb) and backward  $-3.6 < y < -2.6$  (Pb-p) rapidity, thus providing the following energy ranges:  $21 < W_{\gamma p} < 45$  and  $577 < W_{\gamma p} < 952$  GeV.

Figure 1 (left) shows the invariant mass of the selected dimuons for both p-Pb and Pb-p configurations. The fit is performed by a Crystal Ball function [10] for the signal and an exponential function for the background. The parameters of the fit are compatible with the expectations of detailed simulations of the response of the detector to this type of events.

In order to extract the number of exclusive  $J/\psi$  candidates, the  $p_T$  distribution of dimuons within the  $J/\psi$  mass peak (inv. mass  $2.8 < M_{\mu^+\mu^-} < 3.3$  GeV/c<sup>2</sup>) is described by 3 contributing processes, exclusive  $J/\psi$  in  $\gamma p$ ,  $\gamma\gamma \rightarrow \mu^+\mu^-$  and non-exclusive  $J/\psi$ .

The fits to the  $p_T$  distributions are shown in the right part of Figure 1, the shapes for exclusive  $J/\psi$  and  $\gamma\gamma \rightarrow \mu^+\mu^-$  were generated using STARLIGHT [11] and folded with a GEANT3 detector simulation and the contribution of non-exclusive  $J/\psi$  and  $\gamma\gamma \rightarrow \mu^+\mu^-$  was estimated from data.

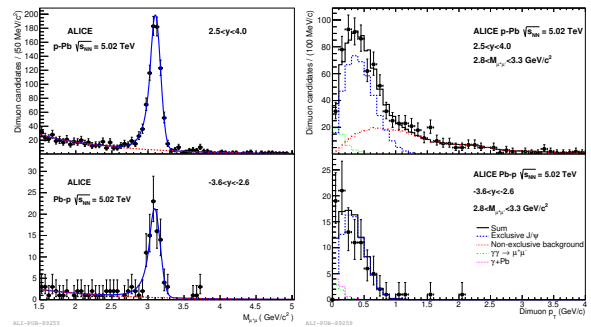


Figure 1: Invariant mass and transverse momentum distributions for forward (up) and backward (down) dimuon samples [9].

## 4. Exclusive $J/\psi$ cross section in p-Pb at $\sqrt{s_{NN}} = 5.02$ TeV

The differential cross section of exclusive  $J/\psi$  production from  $\gamma p$  interactions can be calculated with formula 3 in [7] using the measured number of exclusive  $J/\psi$  candidates, the luminosity and the detection efficiency.

The cross section of  $\gamma p \rightarrow J/\psi + p$  is proportional to the measured differential cross section  $d\sigma/dy$  via the the photon spectrum  $dN_\gamma/dk$ , which is the distribution of photons carrying a momentum  $k$ :

$$\frac{d\sigma}{dy}(\text{p} + \text{Pb}) = k \frac{dN_\gamma}{dk} \sigma(\gamma + \text{p}). \quad (1)$$

<sup>1</sup>Pseudorapidity intervals given in the laboratory frame

114 The average photon flux has been calculated from 143  
115 STARLIGHT.

116 The  $\sigma(\gamma+p)$  cross section measured by ALICE is 144  
117 shown in Figure 2 [9] as a function of  $W_{\gamma p}$ . The upper 145  
118 part of the figure compares the measurement to HERA 146  
119 data [3] [4] and theoretical models, in the lower panel 147  
120 there is a comparison of ALICE results and LHCb solu- 148  
tions extracted from pp data.

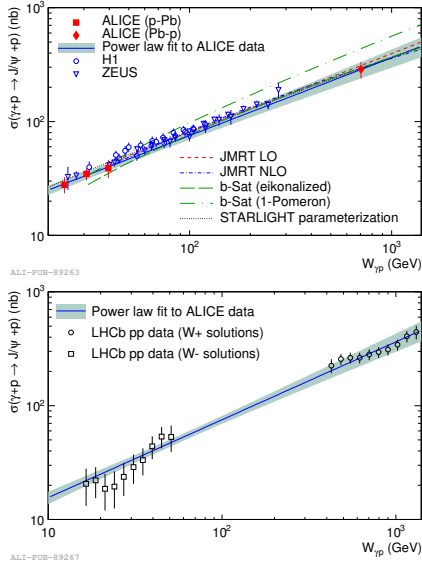


Figure 2: Exclusive  $J/\psi$  photoproduction cross section off protons [9].

121 A power law fit to ALICE data is in agreement with 149  
122 a similar fit to HERA data. The LHCb solutions are 150  
123 consistent with the power law fit obtained from ALICE 151  
124 results. 152  
125

### 126 5. Coherent $J/\psi$ cross section in Pb-Pb at $\sqrt{s_{NN}} =$ 127 2.76 TeV

128 Photoproduction of  $J/\psi$  in Pb-Pb UPC is considered 153  
129 *coherent* in the case of coherent photon coupling to the 154  
130 nucleus, while coupling to a single nucleon leads to the 155  
131 *incoherent* photoproduction.

132 The measurement using the muon spectrometer [7] 156  
133 followed a similar analysis procedure as already de- 157  
134 scribed for the p-Pb case. In addition there was a mea- 158  
135 surement at mid-rapidity [8] based on events with  $\mu^+\mu^-$  159  
136 or  $e^+e^-$  pairs reconstructed in the central tracking sys- 160  
137 tem and no other activity registered in ALICE. Muons 161  
138 and electrons were separated by their specific energy 162  
139 loss in the TPC. 163

140 ALICE results on the coherent  $J/\psi$  cross section are 164  
141 shown in Figure 3 along with different theoretical pre- 165  
142 dictions based on pQCD (AB, RSZ), color dipole model 166  
143 (CSS, GM, LM) or a Glauber approach (STARLIGHT). 167  
144 Calculations by Adeluyi and Bertulani [12] using the 168  
145 EPS09 nuclear prediction is in the best agreement with 169  
146 the measured coherent cross section. 170  
147

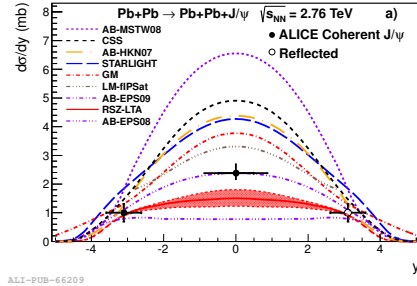


Figure 3: Cross section of coherent  $J/\psi$  photoproduction in Pb-Pb UPC [8].

### 147 6. Conclusions

148 ALICE measurements of  $J/\psi$  photoproduction in 153  
149 ultra-peripheral p-Pb and Pb-Pb collisions (UPC) have 154  
150 been described. Changes in gluon density from HERA 155  
151 to LHC do not affect the  $J/\psi$  photoproduction. The 156  
152 cross section of coherent  $J/\psi$  in Pb-Pb favors models 157  
153 which include nuclear gluon shadowing consistent with 158  
154 the EPS09 parametrization.

### 155 Acknowledgements

156 This work was supported by grant LK11209 of 160  
157 MŠMT ČR.

### 158 References

159 [1] A. J. Baltz et al., Phys. Rept. **458**, 1 (2008)  
160 [2] S. Afanasiev et al. [PHENIX Collaboration], Phys. Lett. B **679**,  
161 321 (2009)  
162 [3] S. Chekanov et al. [ZEUS Collaboration], Eur. Phys. J. C **24**,  
163 345 (2002)  
164 [4] A. Aktas et al. [H1 Collaboration], Eur. Phys. J. C **46**, 585  
165 (2006)  
166 [5] T. Aaltonen et al. [CDF Collaboration], Phys. Rev. Lett. **102**,  
167 242001 (2009)  
168 [6] R. Aaij et al. [LHCb Collaboration], J.Phys. G **41** 055002 (2014)  
169 [7] B. Abelev et al. [ALICE Collaboration], Phys. Lett. B **718**, 1273  
170 - 1283 (2013)  
171 [8] E. Abbas et al. [ALICE Collaboration], Eur. Phys. J. C **73**, 2617  
172 (2013)  
173 [9] B. Abelev et al. [ALICE Collaboration], arXiv:1406.7819 [nucl-  
174 ex], (2014)  
175 [10] J. E. Gaiser, Ph.D. thesis, SLAC-R-255, 1982  
176 [11] STARLIGHT website, <http://starlight.hepforge.org/>  
177 [12] A. Adeluyi and C. A. Bertulani, Phys. Rev. C **85** (2012) 044904